The Holocene

Evidence of moist niches in the Bolivian Andes during the mid-Holocene arid period

Marie-Pierre Ledru, Vincent Jomelli, Laurent Bremond, Teresa Ortuño, Pablo Cruz, Ilham Bentaleb, Florence Sylvestre, Adèle Kuentz, Stephan Beck, Céline Martin, Christine Paillès and Sandrine Subitani

The online version of this article can be found at:
http://hol.sagepub.com/content/early/2013/08/21/0959683613496288

Published by:

$SAGE

http://www.sagepublications.com

Additional services and information for *The Holocene* can be found at:

Email Alerts: http://hol.sagepub.com/cgi/alerts

Subscriptions: http://hol.sagepub.com/subscriptions

Reprints: http://www.sagepub.com/journalsReprints.nav

Permissions: http://www.sagepub.com/journalsPermissions.nav

>> OnlineFirst Version of Record - Aug 21, 2013

What is This?

Evidence of moist niches in the Bolivian Andes during the mid-Holocene arid period

Marie-Pierre Ledru,[1] Vincent Jomelli,[2] Laurent Bremond,[3] Teresa Ortuño,[4] Pablo Cruz,[5] Ilhem Bentaleb,[1] Florence Sylvestre,[6] Adèle Kuentz,[1] Stephan Beck,[7] Céline Martin,[1] Christine Paillès[6] and Sandrine Subitani[3]

Abstract

To examine the climate of the mid-Holocene and early human settings in the Andes when the Altiplano was recording the most arid phase of the Holocene, we analyzed plant-related proxies (pollen, phytoliths, diatoms, stable isotopes) from a sediment core sampled at high elevation in the Eastern Cordillera of Bolivia. Our study was carried out in the wetland of Tiquimani (16°12′06.8″S; 68°3′51.5″W; 3760 m), on a well-known pathway between Amazonia and Altiplano. The 7000-year old record shows a two-step mid-Holocene with a dry climate between 6800 and 5800, followed by a wetter period that lasted until 3200 cal. yr BP. In the Central Andes of Bolivia, a widespread aridity was observed on the Altiplano during the mid-Holocene. However, here, we show that moisture was maintained locally by convective activity from the Amazon lowlands. During the arid interval between 5000 and 4000 yr BP, these niches of moisture produced specific grasslands that may have enabled the survival of an archaic culture of hunter–gatherers on the Puna. This development occurred 2000 years before expansion of quinoa cultivation on the Puna.

Introduction

Environmental changes have always affected populations and their activities in all types of societies (Haug et al., 2003). During the early Holocene, hunter–gatherers in the central Andes were mobile; they designed new artifacts and hunted wild camelids, rodents, and cervidae. During the mid-Holocene, between 7 and 4 kyr BP, independent data from dated human skeletons, rock shelter stratigraphy, and chronology of open-air sites have been interpreted to show that the region became depopulated or altogether abandoned (Nuñez et al., 2002). Sedentarism and the development of agriculture are attested throughout the central Andes after 4 kyr BP (Silverman and Isbell, 2008). The mid-Holocene environmental crisis that occurred in the Andean highlands is attributed to a period of extensive aridity (Baker et al., 2001; Thompson et al., 1995), which put a strain on resources in the region. However, little is known about how hunter–gatherer populations managed to survive: did they migrate to another region or invent strategies to adapt to their new environment? The hypothesized exodus from the Puna region during the peak of aridity has been questioned by both archeologists (Yacobaccio, 2006) and plant geneticists (Harlan, 1971; Hawkes, 1999). First, because the descendants of these hunter–gatherer populations emerged as the most powerful of the archaic states in high-elevation basins, including the Wari, Tiwanaku, and Inca cultures with their respective sociopolitical complexity based on the intensive cultivation of maize (Pearsall, 1989; Silverman and Isbell, 2008). And second, because phytogeographical analyses of the cultivated plants provide evidence for the high central Andes as one of the main centers of the origin of agriculture in the Americas (Harlan, 1971), thus refuting the regional extinction of these plants. During the

Holocene, the altitudinal band formed by the Puna, that is, the Andean grassland located between 3500 and *c*. 5200 m a.s.l., was essential for the supply of resources and enhanced interzonal relationships between cultural groups (Pearsall, 1989; Perry et al., 2006). Between the early and mid-Holocene, significant changes in the behavior of the hunter–gatherers of the Puna are evidenced by a sudden increase in the consumption of camelids that coincided with the drastic decrease in wetlands (Silverman and Isbell, 2008; Yacobaccio, 2006). During this period, the Andean wetlands were crucial for the elaboration of new strategies of alimentation for the groups of hunter–gatherers that were living in these environments. In relation to this topic, we conducted a multiproxy palaeoecology study by the mean of sediment archive. A sediment

[1]Institut des Sciences de l'Evolution de Montpellier (ISEM), France
[2]CNRS Université Paris 1, Laboratoire de Géographie, Meudon, France
[3]Paleoenvironments and chronoecology (PALECO), Ecole Pratique des Hautes Etudes (EPHE), & Centre de Bio-Archéologie et d'Ecologie (UMR5059, CNRS, UM2, EPHE, Montpellier, France
[4]Museo Nacional de Historia Natural, La Paz, Bolivia
[5]CONICET-FUNDANDES, Jujuy, Argentina
[6]UMR CEREGE, Université Aix-Marseille, CNRS, IRD, Collège de France, Aix-en-Provence, France
[7]Herbario Nacional de Bolivia, La Paz, Bolivia

Corresponding author:
Marie-Pierre Ledru, IRD UMR 226, Institut des Sciences de l'Evolution de Montpellier (ISEM) UM2 CNRS IRD, Place Eugène Bataillon cc 061, 34095 Montpellier cedex, France.
Email: marie-pierre.ledru@ird.fr
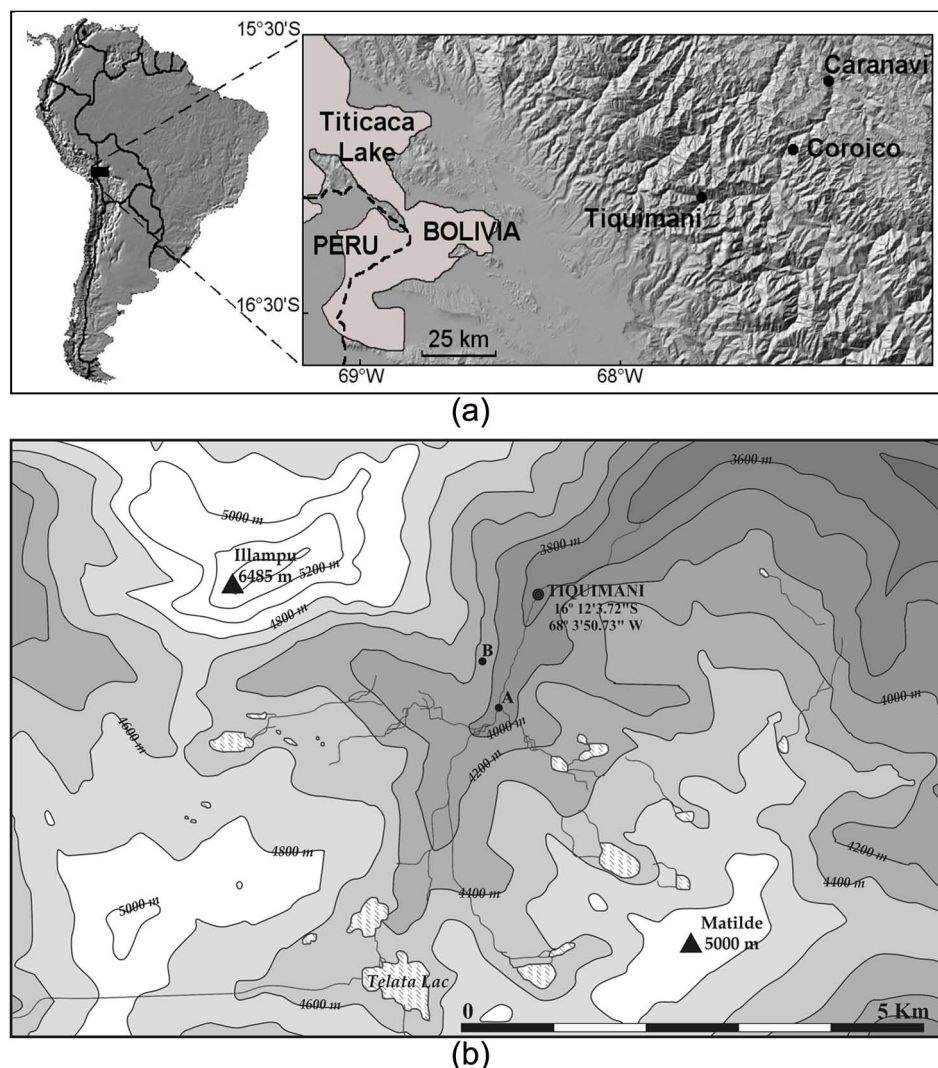
Figure 1. (a) Map showing the altitudinal gradient along a corridor that connects the Amazon basin (Caranavi, 602 m a.s.l.), the city of Coroico (1520 m a.s.l.) to the Altiplano and Lake Titicaca (4200 m a.s.l.) and the location of Tiquimani (3760 m a.s.l.) and (b) location of the wetland of Tiquimani in a narrow pathway, below a glacier (Illampu or Tiquimani).

core covering the last 7 kyr was collected in a wetland of the Puna of the Eastern Cordillera Real in Bolivia. Our interpretations of palaeoenvironmental conditions are based on proxy crossed analysis.

Study site

The Tiquimani wetland (16°12′06,8″ S, 68°3′51,5″ W) is located at an elevation of 3760 m a.s.l. in the Eastern Cordillera Real in Bolivia. This wetland is located in the Puna above a hamlet of five houses whose inhabitants raise pigs and grow quinoa, at the head of an inter-Andean valley today considered to be one of the most accessible trails between Amazonia and Lake Titicaca (Figure 1).

The Puna is composed of shrub steppe Poaceae and halophytic vegetation, along with wetlands that are favorable for the growth of high-quality fodder, and salt marshes. Among the main taxa are Bromeliaceae, *Puya*, Cactaceae, Caryophyllaceae (*Cerastium, Pycnophyllum*), Asteraceae tubuliflorae, Brassicaceae, Cyperaceae, *Geranium*, Poaceae, *Isoetes*, Juncaceae, Lamiaceae, Fabaceae, *Buddleja, Nototriche, Plantago, Ranunculus*, Apiaceae *Azorella*, Valerianaceae, and Violaceae. The upper Andean forest line is located at 3600 m and is characterized by the following taxa Asteraceae tubuliflorae, *Gynoxis, Polylepis, Podocarpus, Ilex, Weinmannia, Ribes*, and Solanaceae (Ortuño et al., 2011).

Today 50% of the annual precipitation of the area of Tiquimani occurs during the austral summer. The climate at Tiquimani is tropical with a wet and a dry season. The wet season, from December to March, is associated with the onset of the South American monsoon and the position of the South Atlantic Convergence Zone (SACZ). During the dry season, from May to August, the occurrence of sparse winter rainfall is associated with the frequency and intensity of cold fronts (Seluchi and Marengo, 2000). The wetland of Tiquimani (3760 m) is located in a pathway corridor that connects Amazon basin to the Altiplano and Lake Titicaca (4200 m a.s.l.), which is close to the Zongo Valley. Studies on climate variability of the Zongo Valley were performed along a transect from the Amazonian lowlands to the Bolivian Altiplano using, in particular, the data of eight rainfall gauges located along the Zongo valley between 1195 and 4750 m a.s.l. (Ronchail and Gallaire, 2006). Results show several altitudinal boundaries in precipitation rates. The maximum of mean annual precipitation (MAP) is observed at 1000 m a.s.l. with 2800 mm. A first decrease, to 2000 mm/yr, is found between 1000 and 1500 m a.s.l and another one up to 1000 mm/yr is measured more than 3000 m a.s.l. On the Altiplano, more than 3900 m a.s.l., MAP drops to 600 mm in the eastern Altiplano and 300 mm in the western Altiplano. El Niño years (cooler sea surface temperature on the Pacific Ocean) result in a 10–20% reduction of MAP in the Zongo valley due to a strong westerly flow above

Table 1. Radiocarbon ages of total organic matter from core TK 1-2. ^{14}C dates are calibrated using CLAM (Blaauw, 2010) with the calibration curve for the Southern Hemisphere SHCal04 (McCormac et al., 2004) and with the Southern Hemisphere postbomb curves from Hua and Barbetti (2004).

Depth (cm)	Lab number	^{14}C age yr BP	Cal. yr BP			δ^{13}C
			Min	Max	Proba %	
2	SacA 3928	−1700	−35.63	−32.07	82.9	−27,800
			−13.25	−12.22	12.1	
10	SacA 3929	2280 ± 50	2122	2343	95	−25,600
18	SacA 3930	3620 ± 50	3697	3984	95	−21,100
24	SacA 3931	5300 ± 35	5919	6032	60	−22,350
			6038	6120	25	
			6148	6178	10	
32	SacA 3932	6070 ± 60	6787	7031	80	−23,600

the Altiplano associated with a weakening and northward displacement of the Bolivian High and prevent the advection aloft of moist air from the Amazon (Garreaud and Aceituno, 2001; Vuille et al., 2000). La Niña events affect the lowland moisture rates and consequently also induce dryness on the eastern cordillera. The modern climatic trend was measured near La Paz and attested an increase of temperatures of 0.03°C/yr and a decrease in relative humidity of 0.6%/yr with the main consequence of retreat of the Zongo glacier of 12 m/yr (Ronchail and Gallaire, 2006).

Methods

The sediment core TK 1-2 was collected in a small wetland in July 2005 with a piston corer. The 36-cm-deep core was sampled at 1-cm intervals (36 samples) at the laboratory of Ecology of the Universidad Mayor de San Andrés (UMSA), La Paz, and every sample divided between the different analyses: pollen, diatoms, phytoliths, and isotopes. Pollen and isotope contents were analyzed first, and samples for phytolith (16 samples) and diatom (10 samples) analyses were selected according to the results obtained with the two first proxies. The same sample was used for each proxy analyzed in core TK 1-2; therefore, the time interval represented by one sample is the same for all the proxies identified within the considered sample.

Chronology

The sediment chronology was based on five radiocarbon accelerator mass spectrometry (AMS) dates. All samples have been analyzed at the Laboratoire de Mesure du Carbone 14 (LMC14) – UMS 2572 (CEA/DSM – CNRS – IRD – IRSN – Ministère de la culture et de la communication) (Table 1). All the radiocarbon ages were calibrated to calendar years Before Present (cal. yr BP) using the calibration curve for the Southern Hemisphere SHCal04 (McCormac et al., 2004) and with the Southern Hemisphere postbomb curves from Hua and Barbetti (2004). Construction of the age–depth model was performed by running the 'CLAM' program (Blaauw, 2010) under the mathematical software 'R' version 2.12.2, and age–depth relationship was estimated using a smooth spline approximation (Figure 2).

Pollen analysis

A total of 36 pollen samples of 0.5 g dry weight each were prepared using a standard treatment (Faegri and Iversen, 1989) and mounted in silicone oil on microscope slides. Pollen analyses were performed under 1000× magnification. Pollen grains and spores were identified using our reference pollen collection and pollen keys (Heusser, 1971; Hooghiemstra, 1984; Markgraf and

D'Antoni, 1978). A minimum of 300 terrestrial pollen grains were analyzed in each sample. Fern spores and aquatic or water-level-related taxa were excluded from the pollen sum for percentage calculation (Appendix). The pollen record was plotted using psimpoll (Bennett, 1994) and divided into five pollen zones on the basis of constrained cluster analysis by sum of squares (CONISS) with pollen taxa ≥1% (Grimm, 1987). Pollen concentration was calculated using the method of Cour (1974).

Isotope analysis

We sampled modern plants and sediments for measurement of carbon stable-isotope and C/N ratios. Four Poaceae species, *Bromus brayacantha, Bromus catharticus* sampled in the Herbarium of La Paz, *Calamagrostis*, and *Festuca* sampled in the field near Tiquimani coring site, and 36 bulk sediment samples were dried at 50°C for 48 h. Leaves and sediment subsamples (1 cm³) were ground using a mortar and pestle and sieved through a 60-μm mesh. For the plants, we used 0.1 mg for C and 1 mg for N analysis. For the carbon and nitrogen analysis, 2 mg and 8 mg bulk sediment powder is weighed, respectively. Plant and sediment powders are introduced in tin capsules prior to elemental and isotope analysis. Elemental C and N contents (%) and carbon isotope values of the plant and sediment were measured by dry combustion using a Euro Vector 3000 Elemental Analyzer coupled with a Micromass Optima Isotope Ratio Mass Spectrometer (ISEM laboratory, Montpellier, France). Results are expressed as a percentage of dry weight (total C and N) and as δ^{13}C with respect to the Vienna Pee Dee Belemnite (V-PDB) standard using the conventional delta (δ) notation: δ (‰) = $[(R_{sample}/R_{standard}) - 1] \times 1000$, where R_{sample} and $R_{standard}$ are the ^{13}C/^{12}C ratios of the sample and standard, respectively. Analytical precision was better than 0.2‰.

Phytolith analysis

Phytoliths were extracted from 16 samples of the Tikimani core. Phytoliths were abundant and well preserved in all the samples. Sediment samples were prepared for phytolith analyses by treatment of 1–2 cm³ (±3 g) of sediments with HCl (33%) to remove carbonates, and then with H_2O_2 (30%) at 70°C to remove organic matter. Clays were deflocculated in a solution of sodium polyphosphate ($NaPO_3$, 0.1%) at pH 7 and removed by centrifugation until the supernatant was clear. Organic silica was separated from the mineral fraction using $ZnBr_2$ heavy liquid at density d=2.30. The residue was removed and rinsed from the filter and dried in glass vials. Slides were prepared using a small amount of dry residue mixed with immersion oil as a mounting medium to allow three-dimensional (3D) observation of the phytoliths during counting. Counting was done at magnification 630×. During
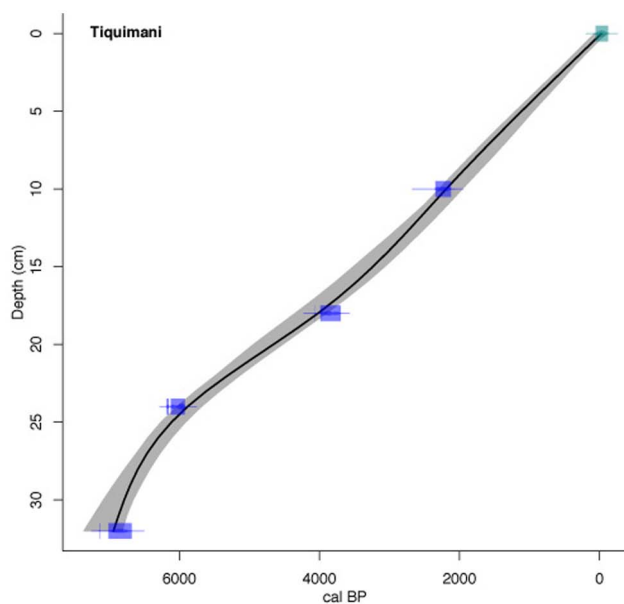
Figure 2. Calibrated age–depth model constructed using CLAM (Blaauw, 2010).

counting, circular to oval phytoliths or 'rondels' (Mulholland, 1989) were differentiated into five types (rondel, stipa-type, horned rondel, truncated rondel, and keeled rondel), but all were summed under generic 'rondel type'. Other shapes not preferentially produced by Bambusoideae/Ehrhartoideae/Pooideae (BEP) grasses (PACCAD clade; Panicoideae, Chloridoideae, Aristidoideae such as bilobates or saddles) were also counted but were present in very low numbers. Phytoliths not produced by short cells and by non-grasses were counted but not used in the calculation of the percentage or in the interpretation.

Diatom analyses

Diatoms were observed in 10 samples and analyzed in 9 samples because in sample of 26–27 cm, the number of diatoms was not high enough to produce a meaningful spectrum. In the 9 samples, diatoms were well preserved except in samples of 14–15 cm and 22–23 cm in which few diatom frustules were found. Diatom taxonomic and counting analyses were conducted on 0.3-g samples and treated using standard procedures (1:1 mixture of H_2O_2 and water, 1:1 mixture of HCl and water), and repeatedly rinsed in distilled water; slides were made using Naphrax high-resolution mountant (Battarbee et al., 2001). For each sample, at least 400 diatom valves were identified and counted using a Nachet NS400 light microscope (differential interference contrast (Normanski) optics, 1000× magnification, numerical aperture (NA) = 1.25). Specimens were identified to their lowest taxonomic level (variety) following Round et al. (1990).

Results and interpretations

Sediment description and chronology

The peat stratigraphy is divided into the following six units with gray silt between 37 and 30 cm, black organic clay between 30 and 28 cm, brown gray clay between 23 and 28 cm, black organic clay between 23 and 18 cm, brown gray clay between 18 and 9 cm, and brown black organic clay between 9 and 0 cm. The age model suggests continuous sedimentation with no evidence of gaps in deposition (Figure 2).

The base of the core dated back to ~7 cal. kyr BP when the wetland began to form after the glacial retreat in the early

Holocene (Jomelli et al., 2011). The gray silt at the base of the core was considered to be a mixture of silt transported and deposited by the glacier after its retreat 7 kyr ago.

Pollen analyses

Differentiation on Poaceae pollen grains is susceptible to bring about relevant ecological issues (Bush, 2002). At Tiquimani, a pollen grain of the Poaceae family was separated because of visible specific morphological features (Figure 3). Exine ornamentation, grain diameter, pore thickness, pore width, and exine thickness were considered to separate the two main types of Poaceae (Table 2). Measurements were performed on the pollen grains to propose a classification in function of the description of the Poaceae in Beug (1961). Our results showed that our pollen is characteristic of a *Bromus* type, which includes the *Bromus* and *Hordeum* genera mentioned in Beug (1961). The undulated surface characteristic of the exine ornamentation is similar to *B. cathartica* described in Salgado-Labouriau and Rinaldi (1990) (Table 2), although the size of the grain is smaller in our fossil record. However, Schüler and Behling (2011) showed that for a same species within the same pollen record sizes of the Poaceae pollen grains differ between different time intervals, for instance, deglaciation versus interglacial, which makes the authors not consider the size as a determinant parameter for fossil material. The second Poaceae pollen type dominates all the pollen spectra (Figure 4) and shows grains with a bigger size and a thinner exine than the *Bromus* type well illustrated on Figure 3. Unfortunately, it was not possible to measure the grains as they were all folded. Our study is based on the fact that a specific pollen type could be distinguished because of both specific morphological patterns and high frequencies at a precise depth of the core.

In addition, the important frequencies of the pollen grains attributed to the group Chenopodiaceae/Amaranthaceae also caught our attention, as this morphological group of taxa is considered as a low pollen producer and disperser. Indeed, a review of published material referring to Andean pollen grains of Chenopodiaceae/Amaranthaceae showed that in general, frequencies never reached more than 2% (Chepstow-Lusty and Winfield, 2000; Correa-Metrio et al., 2010; Hansen et al., 1994; Ortuño et al., 2011), and frequencies increase up to 10% when the pollen record comes from a saline lake (Chepstow-Lusty et al., 2005), which is not the case of our study, or when agricultural conditions are illustrated (Chepstow-Lusty and Winfield, 2000; Kuentz et al., 2012; Sublette Mosblech et al., 2012; Williams et al., 2011). Consequently, we inferred that the increase in Chenopodiaceae/Amaranthaceae pollen frequencies to more than 10% observed at Tiquimani was anthropogenic. In addition, modern descriptions of the pollen grain of quinoa pollen (*Chenopodium quinoa* Willd. (Chenopodiaceae)) by Graf (1992) and Kuentz et al. (2007) in IRD pollen reference collection (Figure 3) allowed the identification of quinoa type in our pollen record. The description of the following pollen zones is based on the results shown on Figure 4.

Zone T-1 (5 samples, 36–28 cm depth, 7–6.8 cal. kyr BP) is characterized by high frequencies of arboreal pollen (AP) (between 20% and 50%) primarily *Podocarpus* with two peaks at 23%, *Alnus* (1–2%), and *Hedyosmum* (7–22%); fern spores *Cyathea* and *Lycopodium* are well represented at more than 150%, and one sample with *Bromus* type 13% was observed at 31 cm. This level represents the base of the core and is characterized by a gray silt poor in organic matter and in pollen content with pollen concentration less than 100 grains/g.

Zone T-2 (5 samples, 28–24 cm depth, 6.8–5.8 cal. kyr BP) is characterized by a decrease in AP frequencies (until 4–10%) and
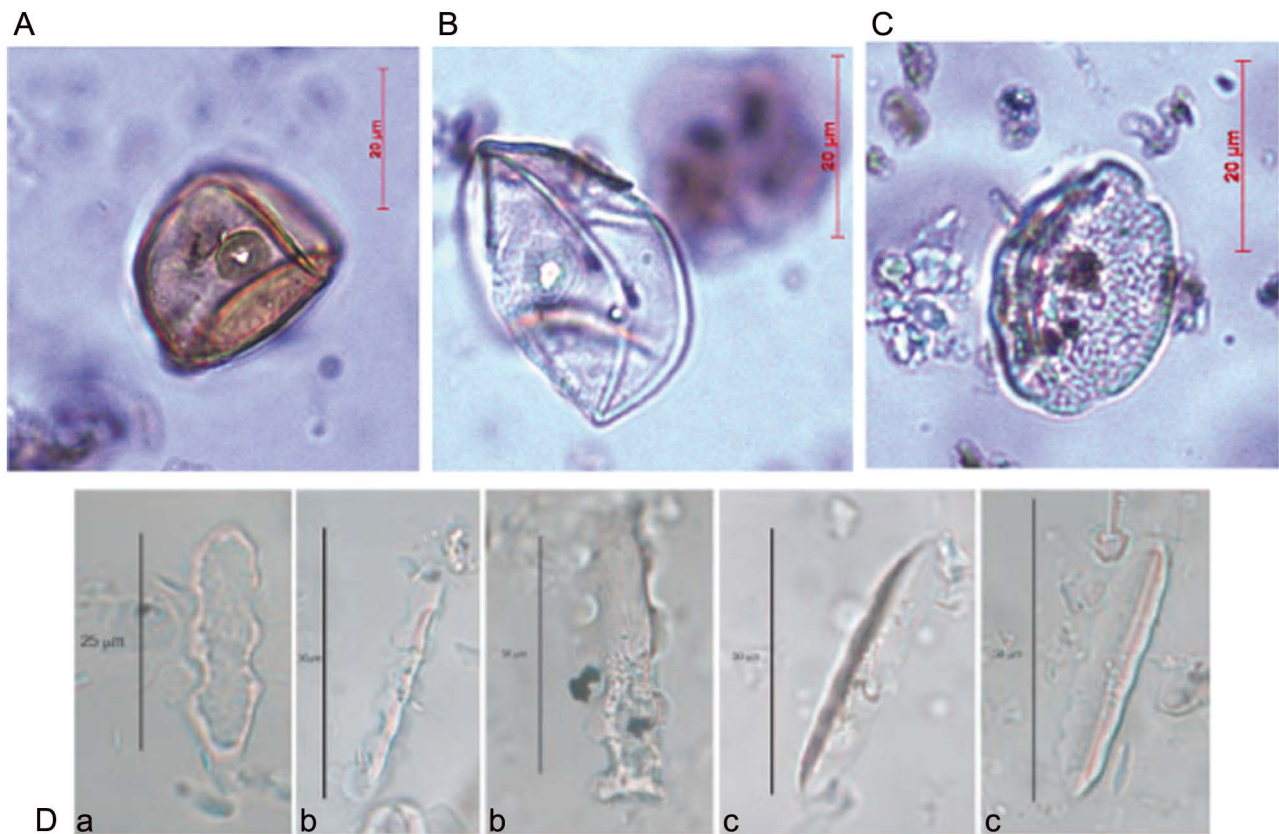
Figure 3. Pictures of the fossil pollen and phytolith identified in sample 18 of Core TK 1-2. (A) *Bromus* type, (B) dominant Poaceae, (C) Chenopodiaceae quinoa type, and (D) long, wavy trapezoid phytoliths produced by Pooideae grasses with (a) *Trapeziform trilobate*, (b) *Trapeziform polylobate*, and (c) wavy trapezoid phytolith (also called *Trapezoid sinuate*) mainly produced by *Bromus* grasses.

Table 2. Measurements of the different Poaceae pollen types. Numbers in bracket refer to the mean value obtained from the measurements.

Plant/pollen taxa	Pore (µm)	Grain diameter (µm)	Exine thickness (µm)
Bromus catharticus M. Vahl	Thickness = 3.5-4 Width = 10	35-41-41-37-41 (39)	1.5-2
Fossil sample 17 cm (8 grains)	Thickness = 5-5-6.5-4.5-5-6.5-5-4.5 (5.25) Width = 15-15-18-15-15-18-15-15 (15.75)	45-45-45-51-60-60-45-35 (48.25)	1.5-1.5-1.5-2-1.5-1-2-2 (1.6)
Fossil sample 18 cm (10 grains)	Thickness = 4-3,5-3 (3.5) Width = 10-10-10-8-10-9-10-10 (9.6)	35-40-31-35-32-30-40 (34.7)	1-1-2-1.5 (1.4)
Fossil sample 19 cm (4 grains)	Thickness = 5-5-6.5-5 (5.3) Width = 15-15-18-15 (15.75)	45-45-60-45 (48.75)	1-1.5-2-1.5 (1.5)
Bromus brachyanthera Döll	Width = 2 Thickness = 2	50-52-53 (52)	Not measured
Hordeum–Bromus type (Beug, 1961)	Width = 2.7-4.0	27.9-47.8-41.1	2.0-2.7
Bromus mango E. Desv. (Heusser, 1971)	Width = 10, distinct annulus Thickness = 1	46-53	Tectate-psilate
Bromus setifolius Presl. (Wingenroth and Heusser, 1983)	Width = 3.7	35.5	Not measured
Hordeum halophilum Gris. (Wingenroth and Heusser, 1983)	Width = 3.6	38.9	Not measured

the presence of an assemblage of Ericaceae (1–6%) and *Piper* (17–30%), and a decrease in fern spores with less 100%. The assemblage of Ericaceae–*Piper* does not exist today, and no *Piper* grows at such a high elevation today (Ricardo Callejas, 2011,

personal communication). Pollen concentration increased to more than 1500 grains/g.

Zone T-3 (7 samples, 24–14 cm depth, 5.8–3.2 cal. kyr BP) is characterized by an increase in AP frequencies (10–30%) primarily
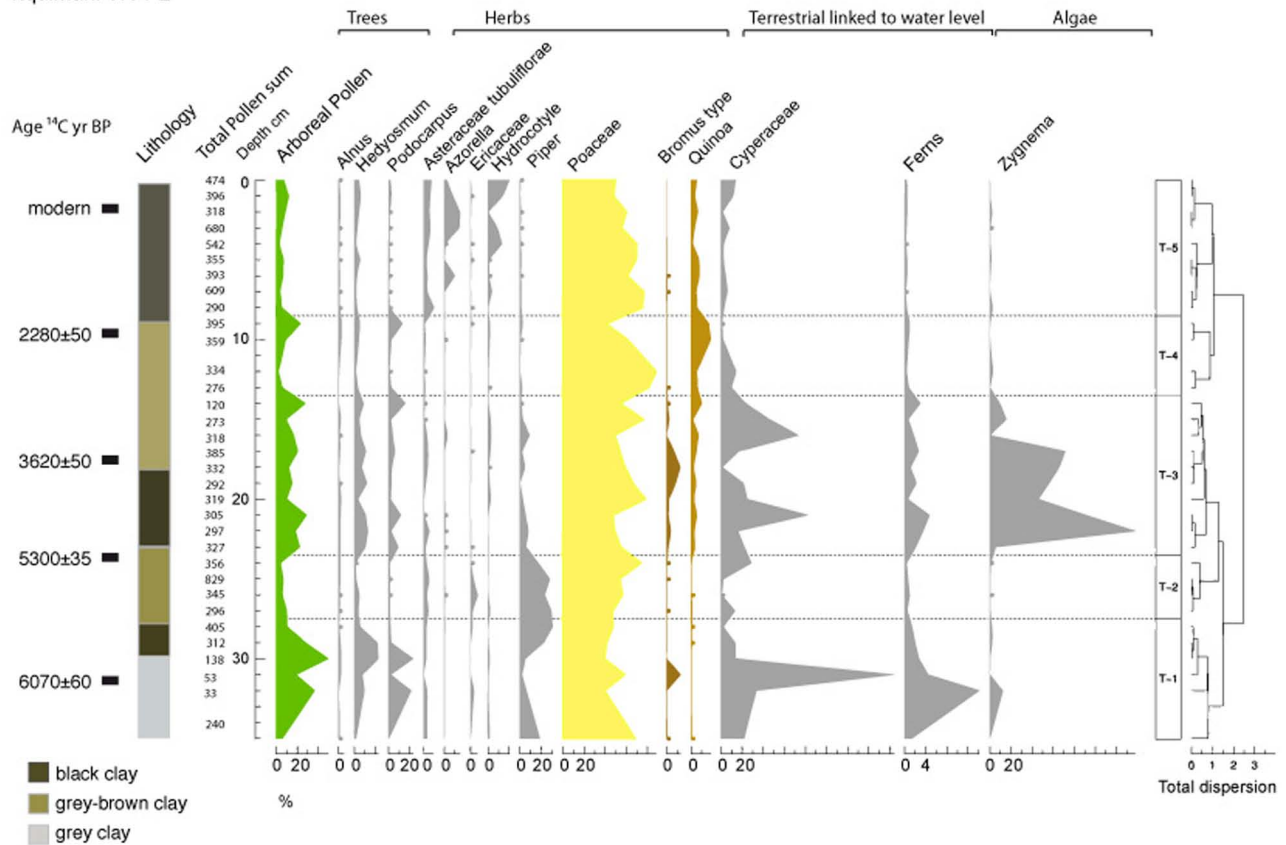
Figure 4. Synthetic pollen diagram of the Tiquimani core TK 1-2. Arboreal pollen frequencies and 14 selected taxa are expressed as percentages of the total pollen sum (excluding ferns) along a depth scale.
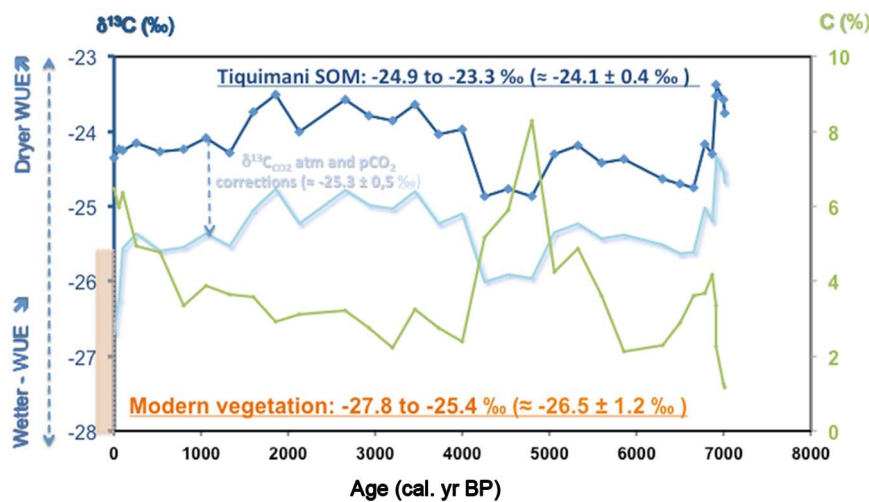
Figure 5. Total organic carbon (%; green solid line) and $\delta^{13}C$ of Tiquimani sediment organic matter core without (dark blue) and with corrections (light blue) (see text). The orange area reflects the $\delta^{13}C$ of modern vegetation at Tiquimani.

Alnus (1–2%), *Hedyosmum* (6–12%), and *Podocarpus* (2–11%); the increase of *Bromus*-type pollen (2–12%), Chenopodiaceae-quinoa (3–5%), Cyperaceae, fern spores, and the algae Zygnemataceae is well represented. The vegetation was more diverse attesting to increased moisture rates both at the edaphic and atmospheric levels. The agriculture of *Bromus* type and quinoa started in the basin during this interval with some irrigation as attested by the presence of Zygnemataceae. In this zone, pollen concentration fluctuated between 200 and 2500 grains/g.

Zone T-4 (5 samples, 14–9 cm depth, 3.2–1.8 cal. kyr BP) is characterized by a progressive decrease in AP frequencies (16–2%)

and high frequencies of quinoa (5–10%). Pollen concentrations remained low, between 500 and 1500 grains/g.

Zone T-5 (11 samples, 9–0 cm depth, 1.8–0 cal. yr BP) is characterized by low frequencies of AP (3–11%), primarily *Hedyosmum* (1–5%). Frequencies of quinoa fluctuated between 18% and 5%. *Azorella* and *Hydrocotyle* both progressively increased in the second half with more than 10% attesting to an open and cold vegetation as the one that grows today at high elevation, also suggested by the decrease in fern spores and Cyperaceae. In this zone, pollen concentration increased more than 3000 grains/g reaching 12,000 grains/g.

Table 3. Plant isotopic composition and nitrogen and carbon contents (*n* is the number of replicates of the same sample and δ¹³C is expressed in ‰).

Locality	Taxa	%C	SD	%N	SD	δ¹³C	SD	C/N
Herbarium of La Paz	*Bromus brayacantha*	42.7 (*n* = 2)	0.3	3.1 (*n* = 2)	0.1	−27.8 (*n* = 2)	0.0	13.9
	Bromus catharticus	41.3 (*n* = 2)	0.2	3.4 (*n* = 2)	0.1	−25.6 (*n* = 1)	–	12.3
Field near Tiquimani	*Calamagrostis sp*	42.0 (*n* = 1)	–	1.4 (*n* = 2)	0.0	−27.3 (*n* = 1)	–	29.5
	Festuca sp	42.6 (*n* = 1)	–	1.2 (*n* = 2)	0.1	−25.4 (*n* = 1)	–	35.8

SD: standard deviation.

Plant and sedimentary organic carbon isotopic composition

Plant. As plants are the primary C sources of soil organic matter (SOM), bulk $\delta^{13}C_{SOM}$ is used as an indicator of the $\delta^{13}C$ of the vegetation and of the abundance of C_3 and C_4 plants (Guillet et al., 2001). $\delta^{13}C$ is a well-established tool used to determine carbon fixation pathways of plant species and plant water-use efficiency (WUE). Indeed, the differences between carboxylation reactions induce disparate photosynthetic ^{13}C fractionation with median values of about −27‰ and −12‰, respectively, for C_3 and C_4 plants. C_3 plants growing under water-stressed conditions are expected to be enriched in ^{13}C compared with plants growing under optimal water conditions (Farquhar and Sharkey, 1982), while the C_4 pathway enables a higher plant-use efficiency (WUE) and a more effective CO_2 uptake, because they use a CO_2 concentrating mechanism (Leegood, 1999) allowing them to grow in climates with low precipitation or slightly saline environments.

$\delta^{13}C$ values of the Poaceae, *B. brayacantha* and *B. catharticus*, sampled in the Herbarium of La Paz and the two most abundant Poaceae, *Calamagrostis* and *Festuca*, sampled in the field near Tiquimani coring site, vary in the same range between −27.8‰ and −25.4‰, all of which follow a C_3 photosynthetic pathway (Table 3). Our isotopic results and field observations suggest that the modern Andean ecosystem is C_3 dominated (>80% of C_3 specimen), also supported by Barberena et al. (2009) who reported values of $\delta^{13}C$ of −28.5‰ and −27.5‰, respectively, for *Bromus* and *Festuca* species sampled on hilltops at 2010 m a.s.l. near Bogota. The difference between our values and those of Barberena et al. (2009) may be partly explained by the altitudinal difference. Indeed, fractionation in C_3 plants is lower at higher altitude (Bird and Pousai, 1997; Körner et al., 1988). The four specimens have also similar amount of carbon content (~42%). However, the nitrogen content is twice higher in *Bromus* type (~3%) compared with the two other species explaining their significantly lower C/N ratios (Table 3). Finally, though the number of modern plant isotopic analyses is limited, we assume that Tiquimani site is likely a C_3-dominated ecosystem with typical values around −26.5‰.

Sediment core. The four sedimentary biogeochemical proxies, $\delta^{13}C_{SOM}$, carbon content, nitrogen content, and C/N ratios, varied, respectively, between −24.9‰ and −23.3‰, 6.5% and 1.2%, 0.6% and 0.1%, and 10% and 16% (Table 3 and Figure 5). At first glance, $\delta^{13}C_{SOM}$ and C/N ratios at Tiquimani suggest a C_3-dominated ecosystem characterized by relatively enriched ^{13}C compared with modern C_3 plant during the past 7 kyr as the mean sediment core $\delta^{13}C_{SOM}$ is about 2‰ heavier than the modern plant (Figure 5). This difference can be explained either by environmental changes or fungi degradation. Indeed, ^{13}C-enrichment occurs during decomposition, and as a result, deep soil organic matter may tend to have higher ^{13}C values than the surface (e.g. Natelhoffer and Fry, 1988; Stout et al., 1981; Stout and Rafter, 1978). Wetland sedimentary organic matter (SdOM) may result

from a complex combination of sources: autochthonous organisms (freshwater food chain) and/or allochthonous material (terrestrial riverine and atmospheric inputs). Hence, the isotopic composition of the SdOM may also reflect a mixture of these diverse sources. At Tiquimani, several hypothesis could be inferred to understand the origin of the SdOM and the causes of the $\delta^{13}C_{SOM}$ variability:

1. The observed covariation between the carbon and nitrogen contents ($R^2 = 0.9$) suggests that C and N of organic matter underwent the same decomposition processes. $\delta^{13}C_{SOM}$ values do not significantly covary with both C ($R^2 = 0.3$, $n = 33$ or $R^2 = 0.2$, $n = 32$) and N ($R^2 = 0.1$) elements, suggesting that the changes of the $\delta^{13}C_{SOM}$ are not heavily affected by the degradation of the sedimentary organic matter stock.
2. Generally, freshwater algae organic matter is characterized by relatively low C/N ratios, while higher values suggest a substantial contribution of terrestrial sources (Sifeddine et al., 2004). Therefore, we assume that organic matter at Tiquimani sediment core is dominated by terrestrial carbon input throughout the past 7 kyr.
3. Stable $\delta^{13}C_{SOM}$ ratios from the surface to ~8 cm (~1300 yr BP) and significant decrease in carbon and nitrogen contents suggest that the decomposition effect on the carbon isotopic fractionation between fresh and decomposed organic matter is low at this site.
4. An alternative interpretation for ^{13}C-enrichment is a change in the balance of the C_3 and C_4 plant and in climate. Indeed $\delta^{13}C$ of C3 plants decrease significantly with increase in precipitation with, for instance, −0.49‰/100 mm (Wang et al., 2003).
5. Modern plants grow under different conditions compared with their preindustrial counterparts that formed the sedimentary organic matter. This may explain the average difference between $\delta^{13}C_{Plant} − \delta^{13}C_{SOM}$ (2.3‰). First, the $\delta^{13}C$ value of atmospheric CO_2 was 1.3‰ higher than it is today (Leuenberger et al., 1992; Marino et al., 1992). Thus, accounting for the first correction, the difference between $\delta^{13}C_{Plant}$ and $\delta^{13}C_{SOM}$ is 1‰. Second, amounts of atmospheric CO_2 between 7 kyr BP and ~0.2 kyr (preindustrial) have increased from ~260 to 280 ppmv and exploded to ~380 ppmv in the late 20th century. These CO_2 concentration levels may also have affected the $\delta^{13}C$ values of C_3 plants (Feng and Epstein, 1995). Assuming this ^{13}C depletion rate, the remaining 1‰ $\delta^{13}C_{Plant} − \delta^{13}C_{SOM}$ difference is explained by a change of ~100 ppmv, which is about the pCO_2 difference between the preindustrial and the early 21st century. The corrected $\delta^{13}C$ curve is given in Figure 5.

Consequently, despite the small amplitude range of the $\delta^{13}C_{SOM}$ values along the core (2.4‰ for the whole corrected curve or 1.7‰, if we do not account for the last 150 years
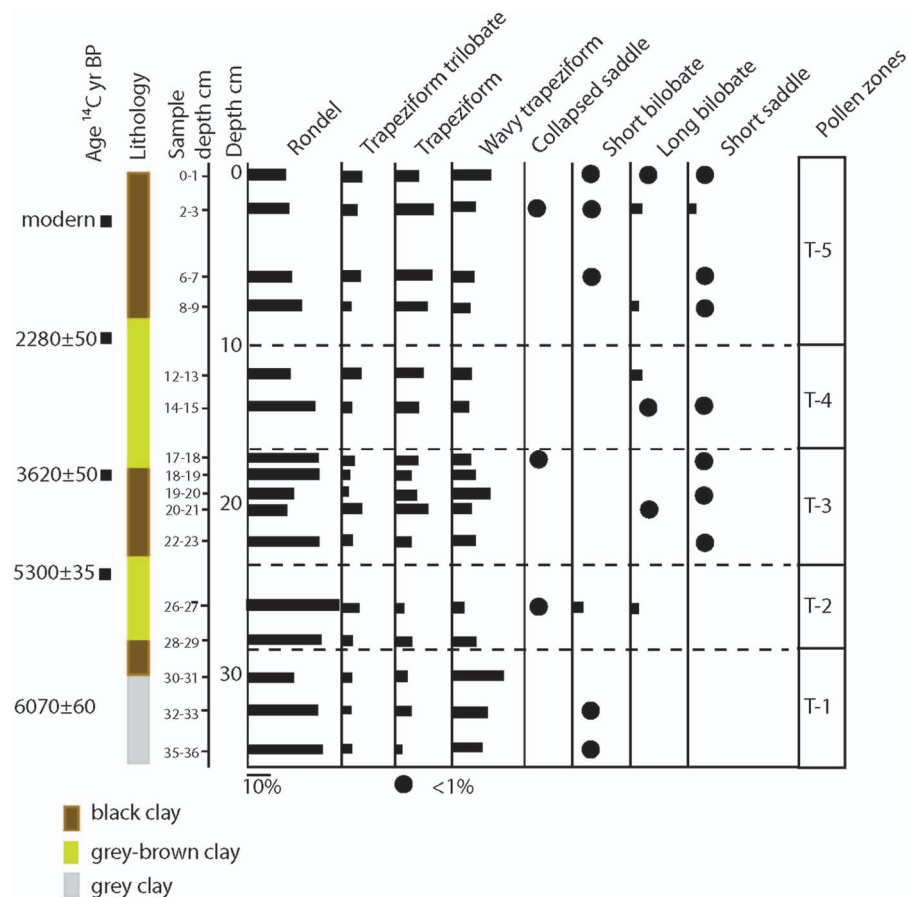
Figure 6. Synthetic phytolith diagram of the Tiquimani TK 1-2 core showing the results for the 16 samples analyzed. The heights of the most common GSSC types are expressed as percentages of the total GSSC sum along a calibrated age scale. Pollen zones from Figure 2 are reported in the diagram.
GSSC: grass silica short cell; WUE: water-use efficiency.

influenced by the anthropogenic activities), we suggest that the $\delta^{13}C_{SOM}$ variations reflect responses of the C_3-dominated ecosystem to precipitation changes. After 5 kyr BP, the $\delta^{13}C_{SOM}$ shift of 0.6‰ is equivalent to about 150 mm (using the Wang et al. (2003) calibration since the relationship is not available for our study area). Between 4 and 1.5 kyr, the higher $\delta^{13}C_{SOM}$ is attributed to a response of the Puna grassland to drier climatic conditions over long intervals. Mean annual precipitation was likely about 200 mm less than today. Plants that thrive under these conditions, like quinoa (see pollen and phytolith discussion), considered to have good drought tolerance (Jensen et al., 2000), are characterized by a relatively high WUE that would explain the high $\delta^{13}C_{SOM}$.

Phytolith analyses

At this altitude, in this region, C_3 grasses are dominant (Bremond et al., 2012; Renvoize, 1998) and BEP grass taxa are most often observed. Particular care was taken to differentiate grass silica short cells (GSSCs) produced by BEP grasses. Moreover, because 'long, wavy trapezoids' appear to be unique to the Pooideae (Barboni and Bremond, 2009; Piperno and Pearsall, 1998), they were differentiated during counting and split into three classes (Figure 3a and b): *Trapeziform trilobate, Trapeziform polylobate* (multilobed short cell; Piperno and Pearsall, 1998) characterized by large lobes, and wavy trapeziform with small lobes (Piperno and Pearsall, 1998), also called Trapeziform sinuate (Figure 3c). This last one is particularly interesting because *Bromus* grasses mainly produce this shape (Blinnikov, 2005; Lu et al., 2006; Morris et al., 2009). The GSSC assemblages are typical of high elevations; BEP phytoliths were dominant

throughout the core, although significant variations were observed. Wavy trapeziform phytoliths always represented more than 15% of the GSSCs but reached higher frequencies at the base of the core, around 4.2 cal. kyr BP, and increased during the last 1500 years (Figure 6). Variations in wavy trapeziform types were interpreted as a change in dominant grass species around the site. Similar pattern in variations in wavy trapeziform and the *Bromus*-type pollen grain frequencies along the core suggested an increase of this Poaceae genus favored by either human activity or climate around 4.2 cal. kyr BP. The background production of wavy trapeziform phytoliths, represented by the minimum of the curve around 15%, can be explained by the production of other grasses due to the phenomena of multiplicity and redundancy (Rovner, 1971). Nevertheless, it cannot be excluded that grasses other than *Bromus* produced this type of phytolith, even during phases with higher frequencies. This is clear for the last 1500 years when no *Bromus*-type pollen grains were identified, and for the modern period when wavy trapeziform phytolith reached 25% of the GSSCs, while *Bromus* grasses were not observed among dominant grasses.

Diatom analyses

From the base up to 19–20 cm, the diatom flora was dominated by benthic, aerophilous, and acidophilous taxa, mainly represented by *Eunotia spp, Pinnularia spp*, and *Luticola mutica* (Figure 7). These taxa are characteristic of high-elevation peat bog soils, and indicate low but constant humidity. At 22–23 cm, an association of two tychoplanktonic taxa, *Aulacoseira perglabra* and *Fragilaria capucina*, were observed. *Fragilaria capucina* shows low
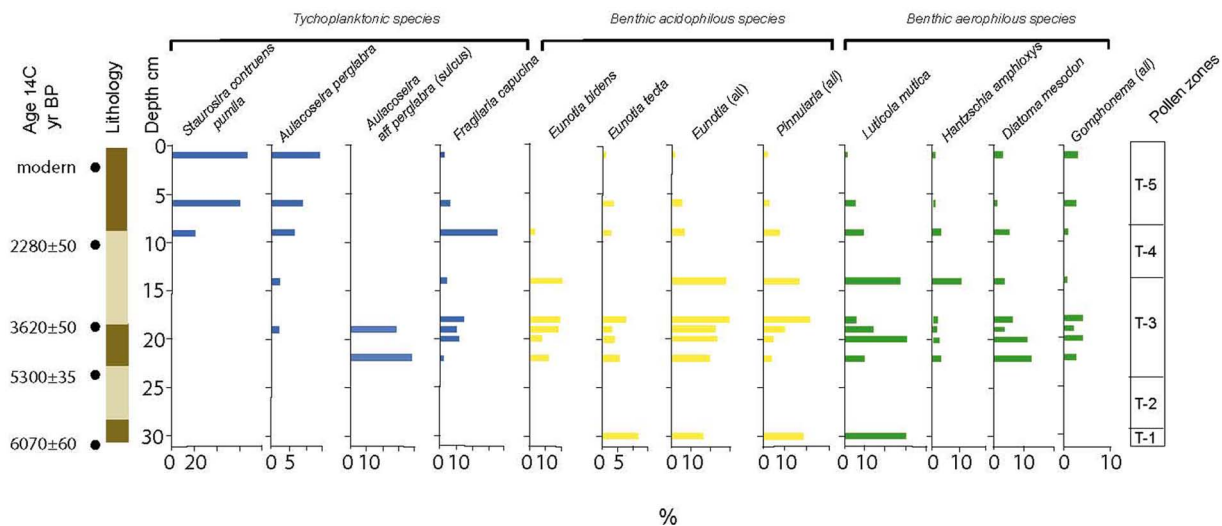
Figure 7. Summary of diatom assemblages from core TK 1-2 showing the results obtained for the 10 samples analyzed. Major diatom species are grouped according to their ecological preferences. Diatoms are expressed in relative abundance (%) along a depth scale. Pollen zones from Figure 2 are reported in the diagram.

frequencies (2%) when *Aulacoseira perglabra* dominates (38%) together with aerophilous and acidophilous benthics (10%) illustrating environmental variability with periodical water supply. *Aulacoseira perglabra* was mainly represented by its internal structure (e.g. sulcus), indicating that these taxa were poorly preserved, but, nevertheless, represented more than 38% of the assemblage. These taxa were present in the middle of the sequence until the 9–10 cm sample in which *Fragilaria capucina* reached its highest percentage (36%). In the same sample, the tychoplanktonics *Staurosira construens* v. *pumila* appeared and dominated the assemblage until the top of the sequence, reaching more than 60%. These tychoplanktonic taxa indicate moister conditions with increased variability of the level of water feeding the peat bog. Permanent moisture conditions start with sample of 9–10 cm when benthics decrease and tychoplanktonics increase.

## Reconstruction of the environmental history of Tiquimani

The analyses revealed two types of plant assemblages, one linked to regional vegetation, the trees or AP, and the other to local plant distribution, the grasses and the algae. A synthetic diagram presents all the bioindicators and the isotopes along a timescale (Figure 8). Between 6.5 and 5.8 cal. kyr BP, the surface released from ice was colonized by bushes of Ericaceae with low AP and fern frequencies (Figure 4). The observation of the following regional increase in moisture rates was based on the high AP observed between 5.8 and 3 cal. kyr BP. The AP pollen content consisted mainly of three representative cloud forest taxa, *Podocarpus*, *Alnus*, and *Hedyosmum* (Figure 4). As the upper treeline of the Andean forest is located 200 m below the site and as it represents the highest elevation since the beginning of the Holocene (Di Pasquale et al., 2008; Moscol Oliveira and Hooghiemstra, 2010), we may assume that these taxa did not grow locally and that the observed increase in AP frequencies was rather due to an increase in pollen transport by the clouds and deposition in the wetland by the raindrops of the convective activity as observed in our modern calibration (Ortuño et al., 2011). This observation is reinforced by the fact that Poaceae pollen grains are uniformly represented throughout the record, confirming to the continuous presence of grassland on the Puna. In addition, the presence of *Bromus*-type pollen grains and of wavy trapezoid phytoliths preferentially produced by *Bromus* grasses (Piperno and Sues, 2005) was observed

between 5.5 and ~3.2 cal. kyr BP, reaching their highest frequencies at 4.2 cal. kyr BP (Figures 4 and 8). The *Bromus* type includes a nutrient-rich perennial native grass of Bolivia (Renvoize, 1998), still used as fodder at lower elevations today but not previously identified in any of the 20 wetland botanical surveys carried out in the Bolivian Puna (Ortuño, in preparation). This grass was accompanied by Zygnemataceae, an algal spore whose presence indicates phases of shallow and mesotrophic fresh water (Van Geel and Van der Hammen, 1978), abundant tychoplanktonic diatoms, indicating moist and highly variable hydrological conditions (particularly the genus *Aulacoseira*, which requires turbulence to survive in the water column (Figure 7) and lower $\delta^{13}C$ ratios of terrestrial organic matter (C/N > 8), which also suggest moist conditions (Figure 8). This combination of several proxies is characteristic of permanent water levels between 5 and 4 kyr BP. Pollen grains of quinoa, a nutritive grain belonging to the Chenopodiaceae family, also called 'pseudo cereal', were first observed at ~5 cal. kyr BP but continued to be observed at low frequencies until 2.7 cal. kyr BP when it became the dominant crop at Tiquimani (Figure 4). After 4 cal. kyr BP, low AP frequencies show a change in the convective activity at Tiquimani while the regional climate became moister (Figure 8) (Baker et al., 2001).

Discussion

Mid-Holocene in the Central Andes: Alternance of dry and wet phases

The content of the gray silt at the base of the core and dated at ~7 cal. kyr BP is interpreted as the first deposit of the sediment that was mixed with the ice in the glacier. Therefore, the pollen content of this sediment could represent the layer of mixed material released after ice melting and not the original vegetation at 7 cal. kyr BP. The mid-Holocene time period, between 6.8 and 5 kyr BP, is characterized by major changes in the hydrological cycles in tropical South America. The drastic decrease of the lake levels on the Altiplano (Argollo and Mourguiart, 2000), the depletion of the glaciers (Jomelli et al., 2011), the deposition of dust in the ice cores (Thompson et al., 1995), archeological gaps in central Brazil (Araujo et al., 2005) and northern Chile (Nuñez et al., 2002), and regression of the tropical forest in central Brazil (Salgado-Labouriau et al., 1998) were associated with a warmer and a drier climate. Changes in the mean position of the Intertropical Convergence Zone (ITCZ) related to the orbital forcing on a
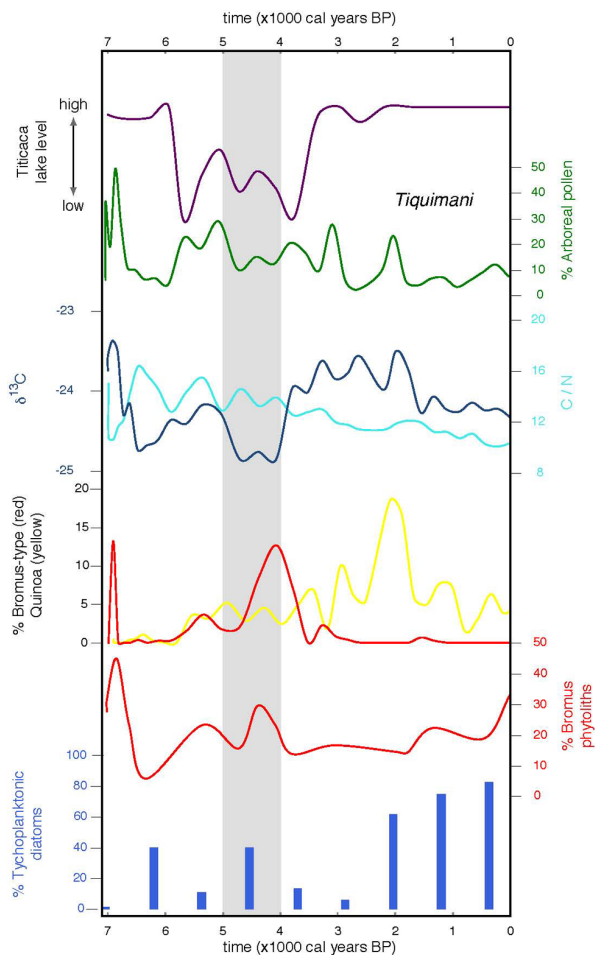
Figure 8. Mid-Holocene climate changes at Lake Titicaca and in the wetland of Tiquimani. The time interval discussed here, between 5000 and 4000 yr BP, is indicated by the gray bar. The low level of Lake Titicaca (Tapia et al., 2003) is compared with high arboreal pollen frequencies deposited by convective activity, changes in stable isotopes pointing to a high plant water-use efficiency, high frequencies of selected pollen of *Bromus* type and of quinoa, high frequencies of wavy trapezoid phytoliths associated with a grass of the *Bromus* group, and high frequencies of tychoplanktonic diatoms characterizing turbulent water at Tiquimani. The timescale was calculated from five radiocarbon dates (Table 1).

millennial timescale and lower summer insolation (Berger and Loutre, 1991) prevented the installation of the rainy season on the continent (Haug et al., 2001). However, differences are observed among the different regions of tropical South America. For instance, the extreme aridity seems rather restricted to the central area in Brazil, the eastern part of the Amazon basin, and the Altiplano. In the Andes, six climate simulations of the mid-Holocene (Jomelli et al., 2011) showed a 0.5°C increase in temperature but also a 0.5 mm/day increase in winter precipitation. These changes were mainly driven by the northward shift of the ITCZ (Braconnot et al., 2007; Vuille and Keimig, 2004), which, in turn, led to a northward shift of the Westerlies and more frequent cold surges in summer and fall at latitude 20°S (Vuille and Keimig, 2004). This feature led to a significant decrease in atmospheric precipitation in the southern tropics documented by the 85-m drop in the level of Lake Titicaca (Baker et al., 2001) (Figure 8) between 7 and 5 kyr BP which, in turn, led to two major dust deposition events in the Cordillera between 5 and 4 cal. kyr BP (Thompson et al., 1995). However, differences in timing and expression of the mid-Holocene aridity are noted according to latitudes. The progressive

re-installation of the ITCZ summer shifts were inferred to explain the observed north–south gradient of the return to wet conditions on the Altiplano and the filling of the lakes between 13°S and 19°S (Abbott et al., 2003). Recently published pollen records showed different expressions of the wet/dry phases during the early to mid-Holocene. At Chochos (7°38′S, 3285 m a.s.l.), a warm interval is observed between 9.5 and 7.3 kyr BP (Bush et al., 2005) and the return to moist conditions is attested after 6 kyr with no fluctuations until today, at Pacucha (13°S, 3095 m a.s.l.) a wet episode is attested from 8.5 until 5 kyr BP followed by drier conditions interrupted by wetter events until today (Hillyer et al., 2009), at Consuelo (13°57′S, 1360 m a.s.l.) dry conditions punctuated by wet phases occurred between 7.4 and 5 kyr BP (Urrego et al., 2010), while Khomer Kocha (17°16′S, 4153 m a.s.l.) characterized the Holocene dry event between 10.1 and 6.4 kyr BP with the maximum of aridity between 7.3 and 7 kyr BP and the return of moisture after 6.4 kyr BP until today (Williams et al., 2011). The increase of humidity observed at Tiquimani (16°S, 3900 m a.s.l.) between 5.8 and 3.2 kyr BP is in agreement with the return to moist conditions observed in the above-cited studies generally after 6 kyr although differences in the expression of the moisture are observed. More to the south in northern Chile and Argentina, alternance of dry and wet periods were observed between 8 and 5.3 kyr BP (Nuñez et al., 2002; Yacobaccio and Morales, 2005).

Origin of moisture

Between 5.8 and 3.2 cal. kyr BP, the observed high arboreal pollen frequencies were transported from trees of the below cloud forest belt and deposited in the wetland by the raindrops of the convective activity. Therefore, based on modern pollen rain studies, the tree pollen frequency could be considered as an indicator of the cloud condensation at this elevation. To explain the mid-Holocene increase in convective precipitation on the Tiquimani wetland, we infer that moisture from the Amazon basin was advected through the valleys to higher elevations where the warm saturated air condenses, producing rainfall on the eastern slope of the Andes (Killeen et al., 2007; Wielicki et al., 2002). The contrast between the warmer and drier climatic conditions observed in Amazonian forests (Mayle and Power, 2008) and the cold and still expanded glacier of the highlands, for instance, Telata (Jomelli et al., 2011), pushed the cloud base up from the lowlands. However, convective activity was not strong enough to allow upward expansion of the cloud forest (Mourguiart and Ledru, 2003). The increase of convective moisture between 5.8 and 3.2 cal. kyr BP did not reach the Altiplano at 4100 m a.s.l. where the climate remained arid until 3800 cal. yr BP. In addition to this convective moisture, intriguing at Tiquimani was the development of a partially inundated grassland between 5 and 4 cal. kyr BP attested by the diatoms, the isotopes, and the presence of fresh algae. At Tiquimani, we suggest that in this particular valley, between the abundance and frequency of clouds (Vuille and Keimig, 2004), the albeit scarce winter precipitation (Haug et al., 2001) and the melting of the glacier above Tiquimani (Jomelli et al., 2011) (5519 m) provided sufficient water to maintain the wetlands during a regional period of aridity. This period between 5.5 and 4 kyr BP, which encompasses the last arid phase and the beginning of the return to moister conditions on the Altiplano (Argollo and Mourguiart, 2000), was crucial for the evolution of Andean societies that had been affected by the scarcity of wetlands (Yacobaccio, 2006). The subsequent expanded cultivation of quinoa in the Puna (Figure 8) provides evidence for another significant step and progressive behavioral modifications of Andean societies when regional moisture returned and a seasonal climate was established in the Eastern Cordillera, driven by the increase in El Niño Southern Oscillation cycles (Moy et al., 2002). These processes were

crucial for the development of the social environment of hunter–gatherers that continued up to the time their descendants became sedentary and established some of the most complex urban centers in human history.

The late Holocene

At 3.2 cal. kyr BP, the ITCZ and the SACZ progressively shifted south to near-modern summer positions with the maximum of insolation centered on the rainy season (Baker et al., 2001).

On the wetland of Tiquimani, the grass was replaced by the quinoa with two maxima of development between 2.3 and 1.8 cal. kyr BP and between 1.3 and 0.8 cal. kyr BP. The development of chenopods after ~2.2 cal. kyr BP is also illustrated in southern Peru and Bolivia (Bruno and Whitehead, 2003; Kuentz et al., 2012; Williams et al., 2011) and characterized a shift in agricultural productions. The quinoa tolerates dry climatic conditions with temperature range between 15° and 4°C (7°C), between 548 and 845 days of rainfall per year, 170 days of frost per year, and a high ultraviolet light exposure due to the high elevation (Del Castillo et al., 2008). Today, two regions are important for the culture of the quinoa, the surroundings of Lake Titicaca and the Uyuni and Lipez Salars, respectively, located in the north and south of Bolivia. The development of the quinoa is coincident with two dry phases at Lake Titicaca when low lake levels were observed between 2.5 and 2.2 cal. kyr BP and at 1.3 cal. kyr BP and were related to changes in the Andean societies (Abbott et al., 1997; Binford et al., 1997). At Tiquimani, the quinoa was progressively abandoned during the last thousand years probably in favor of livestock raising as we can see today.

Conclusion

The record of Tiquimani confirmed the existence of humid spots within the tropical Andes during the so-called arid phase of the mid-Holocene. Our results reveal that the high Andes present a great heterogeneity in climate (Marchant et al., 2001) and landscapes that needs to be observed at finer scales by climatologists, archeologists, and palaeoecologists before being able to understand the origin of many cultivated species that later colonized the Old World and the evolution of the Andean populations, from hunter–gatherer to complex urban societies, which were fully adapted to their environment during the successive wet and dry phases of the Holocene climatic changes. The hypothesis of land abandonment is challenged in favor of changes in practices during the arid period. Our results also highlight the importance of cloud activity as an additional source of moisture transported from the Amazon basin when precipitation becomes scarce during, for instance, a decrease of the seasonal shifts of the ITCZ (González-Carranza et al., 2012; Ledru et al., 2013). The need to improve cloud modeling in the tropics was recently underlined (Wielicki et al., 2002). However, models failed so far to reproduce links between tropical radiative budget and seasonal cloud cover variability because of their coarse resolution (Chen et al., 2002), a key issue to evaluate the multiple origins of Andean water resources for the coming century (Bradley et al., 2006).

Acknowledgements

This research is part of the UR GREAT ICE program at IRD and ANR 2010 BLANC 608-01 ELPASO. All radiocarbon dates were measured at the *Laboratoire de Mesure du Carbone 14* (LMC14) – UMS 2572 (CEA/DSM CNRS IRD IRSN). The authors thank the Bolivian authorities for facilitating our fieldwork in the Zongo Valley and Jaime Argollo for his help during fieldwork. The authors thank Vera Markgraf, Francisco Valdez, and Hugo Yaccobaccio for their comments on an earlier draft of the manuscript.

References

Abbott MB, Binford MW, Brenner M et al. (1997) A 3500 ^{14}C yr high-resolution record of water-level changes in Lake Titicaca, Bolivia/Peru. *Quaternary Research* 47: 169–180.

Abbott MB, Wolfe BB, Wolfe AP et al. (2003) Holocene paleohydrology and glacial history of the central Andes using multiproxy lake sediment studies. *Palaeogeography, Palaeoclimatology, Palaeoecology* 194: 123–138.

Araujo AGM, Neves WA, Pilo LB et al. (2005) Holocene dryness and human occupation in Brazil during the 'Archaic gap'. *Quaternary Research* 64: 298–307.

Argollo J and Mourguiart P (2000) Late Quaternary climate history of the Bolivian Altiplano. *Quaternary International* 72: 37–51.

Baker PA, Seltzer GO, Fritz SC et al. (2001) The history of South American tropical climate for the past 25,000 years from the sedimentary record of Lake Titicaca (Bolivia/Peru). *Science* 291: 640–643.

Barberena R, Gil AF, Neme GA et al. (2009) Stable isotopes and archaeology in southern South America. Hunter-gatherers, pastoralism and agriculture: An introduction. *International Journal of Osteoarchaeology* 19: 204–214.

Barboni D and Bremond L (2009) Phytoliths of East African grasses: An assessment of their environmental and taxonomic significance based on floristic data. *Review of Palaeobotany and Palynology* 158: 29–41.

Battarbee RW, Jones VJ, Flower RJ et al. (2001) Diatoms. In: Smol JP, Birks HJB and Last WM (eds) *Tracking Environmental Change Using Lake Sediments: Terrestrial, Algal, and Siliceous Indicators*, vol. 3. Dordrecht: Kluwer Academic Publishers, pp. 155–202.

Bennett KD (1994) 'psimpoll' version 2.23: A C program for analysing pollen data and plotting pollen diagrams (INQUA Commission for the study of the Holocene). *INQUA Working Group on Data-Handling Methods, Newsletter*, January, vol. 11, pp. 4–6.

Berger A and Loutre M-F (1991) Insolation values for the climate of the last 10 million of years. *Quaternary Science Reviews* 10: 297–317.

Beug HJ (1961) *Leitfaden der Pollenbestimmung*. Stuttgart: Gustav Fischer.

Binford MW, Kolata AL, Brenner M et al. (1997) Climate variation and the rise and fall of an Andean civilization. *Quaternary Research* 47: 235–248.

Bird MI and Pousai P (1997) Variations of δ^{13}C in the surface soil organic carbon pool. *Global Biogeochemical Cycles* 11(2): 313–322.

Blaauw M (2010) Methods and code for 'classical' age-modelling of radiocarbon sequences. *Quaternary Geochronology* 5: 512–518.

Blinnikov MS (2005) Phytoliths in plants and soils of the interior Pacific Northwest, USA. *Review of Palaeobotany and Palynology* 135: 71–98.

Braconnot P, Otto-Bliesner B, Harrison S et al. (2007) Results of PMIP2 coupled simulations of the mid-Holocene and last glacial maximum – Part 1: Experiments and large-scale features. *Climate of the Past* 3: 261–277.

Bradley RS, Vuille M, Diaz HF et al. (2006) Threats to water supplies in the tropical Andes. *Science* 312: 1755–1756.

Bremond L, Boom A and Favier C (2012) Neotropical C_3/C_4 grass distributions – Present, past and future. *Global Change Biology* 18: 2324–2334.

Bruno MC and Whitehead WT (2003) Chenopodium cultivation and Formative period agriculture at Chiripa, Bolivia. *Latin American Antiquity* 14: 339–355.

Bush MB (2002) On the interpretation of fossil poaceae pollen in the lowland humid neotropics. *Palaeogeography, Palaeoclimatology, Palaeoecology* 177: 5–17.

Bush MB, Hansen BCS, Rodbell DT et al. (2005) A 17 000-year history of Andean climate and vegetation change from Laguna de Chochos, Peru. *Journal of Quaternary Science* 20: 703–714.

Chen J, Carlson BE and Del Genio AD (2002) Evidence for strengthening of the tropical general circulation in the 1990s. *Science* 295: 838–841.

Chepstow-Lusty A and Winfield M (2000) Inca agroforestry: Lessons from the past. *AMBIO: A Journal of the Human Environment* 29: 322–328.

Chepstow-Lusty A, Bush M, Frogley MR et al. (2005) Vegetation and climate change on the Bolivian Altiplano between 108,000 and 18,000 yr ago. *Quaternary Research* 63: 90–98.

Correa-Metrio A, Cabrera KR and Bush MB (2010) Quantifying ecological change through discriminant analysis: A paleoecological example from the Peruvian Amazon. *Journal of Vegetation Science* 21: 695–704.

Cour P (1974) Nouvelles techniques de détection des flux et des retombées polliniques. *Pollen et Spores* 16: 103–141.

Del Castillo C, Mahy G and Winkel T (2008) La quinoa en Bolivie: une culture ancestrale devenue culture de rente 'bio-équitable'. *Biotechnology, Agronomy, Society and Environment* 12: 421–435.

Di Pasquale G, Marziano M, Impagliazzo S et al. (2008) The Holocene treeline in the northern Andes (Ecuador): First evidence from soil charcoal. *Palaeogeography, Palaeoclimatology, Palaeoecology* 259: 17–34.

Faegri K and Iversen J (1989) *Textbook of Pollen Analysis*. London: John Wiley & Sons.

Farquhar GD and Sharkey TD (1982) Stomatal conductance and photosynthesis. *Annual Review of Plant Physiology and Plant Molecular Biology* 33: 317–345.

Feng X and Epstein S (1995) Carbon isotopes of trees from arid environments and implications for reconstructing atmosphere CO_2 concentration. *Geochimica et Cosmochimica Acta* 59(12): 2599–2608.

Fernandez Honaine M, Zucol AF and Osterrieth M (2006) Phytolith assemblages and systematic associations in grassland species of the south-eastern Pampean plains, Argentina. *Annals of Botany* 98: 1155–1165.

Garreaud RD and Aceituno P (2001) Interannual rainfall variability over the South American Altiplano. *Journal of Climate* 14: 2779–2789.

González-Carranza Z, Hooghiemstra H and Vélez MI (2012) Major altitudinal shifts in Andean vegetation on the Amazonian flank show temporary loss of biota in the Holocene. *The Holocene* 22: 1227–1241.

Graf K (1992) *Pollendiagramme aus den Anden: Eine Synthese zur Klimageschichte und Vegetationsentwicklung seit der letzten Eiszeit*. Zurich: Universität Zurich.

Grimm E (1987) CONISS: A FORTRAN 77 program for stratigraphically constrained cluster analysis by the method of incremental sum of squares. *Computers & Geosciences* 13: 13–35.

Guillet B, Achoundong G, Happi JY et al. (2001) Agreement between floristic and soil organic carbon isotope (C-13/C-12, C-14) indicators of forest invasion of savannas during the last century in Cameroon. *Journal of Tropical Ecology* 17: 809–832.

Hansen BCS, Seltzer GO and Wright HE Jr (1994) Late Quaternary vegetational change in the central Peruvian Andes. *Palaeogeography, Palaeoclimatology, Palaeoecology* 109: 263–285.

Harlan JR (1971) Agricultural origins: Centers and non centers. *Science* 174: 468–474.

Haug GH, Günther D, Peterson LC et al. (2003) Climate and the collapse of Maya civilization. *Science* 299: 1731–1735.

Haug GH, Hughen KA, Sigman DM et al. (2001) Southward migration of the Intertropical Convergence Zone through the Holocene. *Science* 293: 1304–1306.

Hawkes JG (1999) The evidence for the extent of N.I. Vavilov's new world Andean centres of cultivated plant origins. *Genetic Resources and Crop Evolution* 46: 163–168.

Heusser CJ (1971) *Pollen and Spores of Chile, Modern Types of the Pteridophyta, Gymnospermae, and Angiospermae*. Tucson, AZ: The University of Arizona Press.

Hillyer R, Valencia BG, Bush MB et al. (2009) A 24,700-yr paleolimnological history from the Peruvian Andes. *Quaternary Research* 71: 71–82.

Hooghiemstra H (1984) *Vegetational and Climatic History of the High Plain of Bogotá, Colombia: A Continuous Record of the Last 3.5 Million Years*. Vaduz: J. Cramer.

Hua Q and Barbetti M (2004) Review of tropospheric bomb radiocarbon data for carbon cycle modelling and age calibration purposes. *Radiocarbon* 46: 1273–1298.

Jensen CR, Jacobsen SE, Andersen MN et al. (2000) Leaf gas exchange and water relation characteristics of field quinoa (*Chenopodium quinoa* Willd.) during soil drying. *European Journal of Agronomy* 13: 11–25.

Jomelli V, Khodri M, Favier V et al. (2011) Irregular tropical glacier retreat over the Holocene driven by progressive warming. *Nature* 474: 196–199.

Killeen TJ, Douglas M, Consiglio T et al. (2007) Dry spots and wet spots in the Andean hotspot. *Journal of Biogeography* 34: 1357–1373.

Körner C, Farquhar GD and Roksandic Z (1988) A global survey of carbon isotope discrimination in plants from high altitude. *Oecologia* 74: 623–632.

Kuentz A, Galan De Mera A, Ledru M-P et al. (2007) Phytogeographical data and modern pollen rain of the Puna belt in southern Peru (Nevado Coropuna, Western Cordillera). *Journal of Biogeography* 34: 1762–1776.

Kuentz A, Ledru M-P and Thouret JC (2012) Environmental changes in the highland of the western Andean Cordillera (south Peru) during the Holocene. *The Holocene* 22: 1215–1226.

Ledru M-P, Jomelli V, Samaniego P et al. (2013) The Medieval Climate Anomaly and the Little Ice Age in the Eastern Ecuadorian Andes. *Climate of the Past* 9: 307–321.

Leegood RC (1999) Carbon dioxide concentrating mechanisms. In: Lea PJ and Leegood RC (eds) *Plant Biochemistry and Molecular Biology*. 2nd Edition. Chichester: Wiley, pp. 51–79.

Leuenberger M, Siegenthaler U and Langway CC (1992) Carbon isotope composition of atmospheric CO_2 during the last ice age from an Antarctic ice core. *Nature* 357(6385): 488–490.

Lu H-Y, Wu N-Q, Yang X-D et al. (2006) Phytoliths as quantitative indicators for the reconstruction of past environmental conditions in China I: Phytolith-based transfer functions. *Quaternary Science Reviews* 25: 945–959.

McCormac FG, Hogg AG, Blackwell PG et al. (2004) SHCal04 Southern Hemisphere calibration, 0–11.0 cal. kyr BP. *Radiocarbon* 46: 1087–1092.

Marchant R, Behling H, Carlos BJ et al. (2001) Mid- to Late-Holocene pollen-based biome reconstructions for Colombia. *Quaternary Science Reviews* 20: 1289–1308.

Marino BD, McElroy MB, Salawitch RJ et al. (1992) Glacial-to-interglacial variations in the carbon isotopic composition of atmospheric CO_2. *Nature* 357(6385): 461–466.

Markgraf V and D'Antoni HL (1978) *Pollen Flora of Argentina: Modern Spore and Pollen Types of Pteridophyta, Gymnospermae, and Angiospermae*. Tucson, AZ: The University of Arizona Press.

Mayle FE and Power MJ (2008) Impact of a drier Early–Mid-Holocene climate upon Amazonian forests. *Philosophical Transactions of the Royal Society B: Biological Sciences* 363: 1829–1838.

Morris LR, Baker FA, Morris C et al. (2009) Phytolith types and type-frequencies in native and introduced species of the sagebrush steppe and pinyon-juniper woodlands of the Great Basin, USA. *Review of Palaeobotany and Palynology* 157: 339–357.

Moscol Oliveira M and Hooghiemstra H (2010) Three millennia upper forest line changes in northern Ecuador: Pollen records and altitudinal vegetation distributions. *Review of Palaeobotany and Palynology* 163: 113–126.

Mourguiart P and Ledru M-P (2003) Last glacial maximum in an Andean cloud forest (Eastern Cordillera, Bolivia). *Geology* 31: 195–198.

Moy CM, Seltzer GO, Rodbell DT et al. (2002) Variability of El Niño/Southern Oscillation activity at millennial timescales during the Holocene epoch. *Nature* 420: 162–165.

Mulholland SC (1989) Phytolith shape frequencies in North Dakota grasses: A comparison to general patterns. *Journal of Archaeological Science* 16: 489–511.

Natelhoffer KJ and Fry B (1988) Controls on natural Nitrogen-15 and Carbon-13 abundances in forest soil organic matter. *Soil Science Society of America Journal* 52(6): 1633–1640.

Nuñez L, Grosjean M and Cartagena I (2002) Human occupations and climate change in the Puna de Atacama, Chile. *Science* 298: 821–824.

Ortuño T, Ledru M-P, Cheddadi R et al. (2011) Modern pollen rain, vegetation and climate in the Bolivian ecoregions. *Review of Palaeobotany and Palynology* 165: 61–74.

Pearsall DM (1989) Adaptation of prehistoric hunter-gatherers to the high Andes: The changing role of plant resources. In: Harris DR and Hillman GC (eds) *Foraging and Farming: The Evolution of Plant Exploitations*. London: Unwin Hyman, pp. 318–332.

Perry L, Sandweiss DH, Piperno DR et al. (2006) Early maize agriculture and interzonal interaction in southern Peru. *Nature* 440: 76–79.

Piperno DR and Pearsall DM (1998) The silica bodies of tropical American grasses: Morphology, taxonomy, and implications for grass systematics and fossil phytolith identification. *Smithsonian Contributions to Botany* 85: 1–40.

Piperno DR and Sues H (2005) Dinosaurs dined on grass. *Science* 310: 1126–1128.

Renvoize SA (1998) *Gramineas de Bolivia*. London: Royal Botanic Gardens, Kew.

Ronchail J and Gallaire R (2006) ENSO and rainfall along the Zongo valley (Bolivia), from the Altiplano to the Amazon basin. *International Journal of Climatology* 26: 1223–1236.

Round FE, Crawford RM and Mann DG (1990) *The Diatoms: Biology & Morphology of the Genera*. Cambridge: Cambridge University Press.

Rovner I (1971) Potential of opal phytoliths for use in paleoecological Reconstruction. *Quaternary Research* 1: 343–359.

Salgado-Labouriau ML and Rinaldi M (1990) Palynology of gramineae of the Venezuelan mountains. *Grana* 29: 119–128.

Salgado-Labouriau ML, Barberi M, Ferraz-Vicentini KR et al. (1998) A dry climatic event during the Late Quaternary of tropical Brazil. *Review of Palaeobotany and Palynology* 99: 115–130.

Schüler L and Behling H (2011) Characteristics of Poaceae pollen grains as a tool to assess palaeoecological grassland dynamics in South America. *Vegetation History and Archaeobotany* 20: 97–108.

Seluchi ME and Marengo JA (2000) Tropical-midlatitude exchange of air masses during summer and winter in South America: Climatic aspects and examples of intense events. *International Journal of Climatology* 20: 1167–1190.

Sifeddine A, Wirrmann D, Albuquerque AL et al. (2004) Bulk composition of sedimentary organic matter used in palaeoenvironmental reconstructions: Examples from the tropical belt of South America and Africa. *Palaeogeography, Palaeoclimatology, Palaeoecology* 214: 41–53.

Silverman H and Isbell WH (2008) *Handbook of South American Archaeology*. New York: Springer.

Stout JD and Rafter TA (1978) The $^{13}C/^{12}C$ isotopic ratios of some New Zealand tussock grassland soils. In: Robinson BW (ed.) *Stable Isotopes in the Earth Sciences*. Wellington, New Zealand: DSIR Bull 220:75–83.

Stout JD, Goh KM and Rafter TA (1981) Chemistry and turnover of naturally occurring resistant organic compounds in soil. In: Paul EA and Ladd JN (eds) *Soil Biochemistry, Vol 5*. New York: Marcel Dekker, Inc, pp 1–73.

Sublette, Mosblech NA, Chepstow-Lusty A, Valencia BG et al. (2012) Anthropogenic control of Late-Holocene landscapes in the Cuzco region, Peru. *The Holocene* 22: 1361–1372.

Tapia PM, Fritz SC, Baker PA et al. (2003) A Late Quaternary diatom record of tropical climatic history from Lake Titicaca (Peru and Bolivia). *Palaeogeography, Palaeoclimatology, Palaeoecology* 194: 139–164.

Thompson LG, Mosley-Thompson E, Davis ME et al. (1995) Late Glacial stage and Holocene tropical ice core records from Huascarán, Peru. *Science* 269: 46–50.

Urrego DH, Bush MB and Silman MR (2010) A long history of cloud and forest migration from Lake Consuelo, Peru. *Quaternary Research* 73: 364–373.

Van Geel B and Van der Hammen T (1978) Zygnemataceae in quaternary Colombian sediments. *Review of Palaeobotany and Palynology* 25: 377–391.

Vuille M and Keimig F (2004) Interannual variability of summertime convective cloudiness and precipitation in the central Andes derived from ISCDP-B3 data. *Journal of Climate* 17: 3334–3348.

Vuille M, Bradley RS and Keimig F (2000) Interannual climate variability in the Central Andes and its relation to tropical Pacific and Atlantic forcing. *Journal of Geophysical Research* 105: 12447–12460.

Wang GA, Han JM and Liu TS (2003) The carbon isotopic composition of C_3 herbaceous plants in loess area of North China. *Science in China – Series D: Earth Sciences* 46(10): 1069–1076.

Wielicki BA, Wong T, Allan RP et al. (2002) Evidence for large decadal variability in the tropical mean radiative energy budget. *Science* 295: 841–844.

Williams JJ, Gosling WD, Brooks SJ et al. (2011) Vegetation, climate and fire in the eastern Andes (Bolivia) during the last 18,000 years. *Palaeogeography, Palaeoclimatology, Palaeoecology* 1–2: 115–126.

Yacobaccio HD (2006) Intensificacion economica y complejidad social en cazadores-recolectores surandinos. *Boletin de Arqueologia PUCP* 10: 305–320.

Wingenroth M and Heusser CJ (1983) *Pollen of the High Andean Flora. Quebrada Benjamin Matienzo, Mendoza, Argentina*. IANIGLA, Mendoza, Argentina.

Yacobaccio HD and Morales M (2005) Mid-Holocene environment and human occupation of the Puna (Susques, Argentina). *Quaternary International* 132: 5–14.

Appendix

List of the pollen taxa identified in core TK 1-2

Arboreal pollen	*Ambrosia*	*Solanum*	Onagraceae
Adesmia	Annonaceae	Geraniaceae	**Ferns**
Alchornea	Apocynaceae	Gesneriaceae	*Acrostichum*
Alnus	*Apodanthera cucurbitac*	*Gomphrena*	*Adiantum*
Andira type	Asteraceae tubuliflorae	*Gunnera*	*Anemia* type
Araliaceae	Asteraceae liguliflorae	*Hydrocotyle*	*Asplenium*
Arecaceae	Asteraceae *Loricaria* type	*Hyptis*	*Athyrium*
Astronium	Asteraceae *Diplostephium*	Juncaceae	Bryophytes
Casearia	Asteraceae *Chuquiragua*	Loranthaceae	*Cyathea*
Cecropia	Asteraceae *Lasiocephalus*	*Lupinus*	*Cyathea horrida*
Celtis type	Asteraceae *Ophryoglossus*	Malvaceae	*Cystopteris* type
Cupressaceae	Scrophulariaceae	*Montia*	*Grammitis*
Hedyosmum	*Azorella*	*Oxalis*	Huperzia
Hypericum	*Begonia*	*Peperomia*	Hymenephyllaceae
Ilex	*Bocconia Papaveraceae*	Poaceae	*Hypolepis* type
Juglans	*Bomarea*	*Polygonum*	*Isoetes*
Melastomataceae	*Borreria*	*Piper*	*Jamesonia*
Meliaceae/Sapotaceae	Brassicaceae	*Plantago*	Lycopodiaceae
Mimosaceae	Bromeliaceae	*Polygala*	*Melpomene*
Moraceae/Urticaceae	*Bromus* type	*Ranunculus*	*Mesea*
Myrica	*Calceolaria*	Rubiaceae	Monolete
Myrsine	Campanulaceae	*Rumex*	*Ophioglossum*
Myrtaceae	Caryophyllaceae	*Saurauia*	Polypodiaceae
Podocarpus	Chenop-quinoa	*Saxifraga*	*Pteris*
Pouteria	Convolvulaceae	*Solanum*	cf. *Schizaea*
Protium	*Croton*	*Thalictrum*	*Selaginella*
Rosaceae	*Cuphea*	Urticales	*Sphagnum*
Ribes	*Dalea* type	*Valeriana*	*Thelypteris*
Styrax	*Daphnopsis*	*Vicia*	Trilete
Trema	Ericaceae	*Viola*	**Algae**
Vallea	*Escallonia*	**Aquatics or water level–related taxa**	*Zygnema*
Verbenaceae	*Evolvulus*	Alismataceae	
Weinmannia	*Galium*	Cyperaceae	
Non-arboreal pollen	Gentianaceae	Iridaceae	
Acalypha	*Gentianella*	Liliaceae	